Acta Crystallographica Section C
Crystal Structure Communications
ISSN 0108-2701

Hydrogen-bonded assemblies of 5,10,15,20-tetrakis(4-hydroxyphenyl)-porphyrin with dimethylformamide, dimethylacetamide and water

Sophia Lipstman and Israel Goldberg*

School of Chemistry, Sackler Faculty of Exact Sciences, Tel-Aviv University, Ramat-Aviv, 69978 Tel-Aviv, Israel
Correspondence e-mail: goldberg@post.tau.ac.il

Received 11 November 2008
Accepted 27 November 2008
Online 6 December 2008

The title free base porphyrin compound forms hydrogen-bonded adducts with *N*,*N*-dimethylformamide, $C_{44}H_{30}N_4O_4\cdot 4C_3H_7NO$, (I), a mixture of *N*,*N*-dimethylformamide and water, $C_{44}H_{30}N_4O_4\cdot 4C_3H_7NO\cdot H_2O$, (II), and a mixture of *N*,*N*-dimethylacetamide and water, $C_{44}H_{30}N_4O_4\cdot 6C_3H_7NO\cdot 2H_2O$, (III). Total solvation of the four hydroxy functions of the porphyrin molecules characterizes all three compounds, thus preventing its supramolecular association into extended network architectures. In (I), the asymmetric unit consist of two five-component adduct species, while in (III), the nine-component entities reside on centres of inversion. This report provides the first structural characterizations of the free base tetra(hydroxyphenyl)porphyrin. It also demonstrates that the presence of strong Lewis bases, such as dimethylformamide or dimethylacetamide, in the crystallization mixture prevents direct supramolecular networking of the porphyrin ligands *via* O—H···O—H hydrogen bonds, due to their competing O—H···N(base) interaction with the hydroxy functions. The crystal packing of compounds (I)–(III) resembles that of other hydrogen-bonding-assisted tetraarylporphyrin clathrates.

Comment

Porphyrin macrocycles tetrasubstituted with 4-hydroxyphenyl groups at their *meso* positions (TOHPP) provide a classical example of an organic molecule with multiple complementary terminal functional groups directed at four diverging directions of the equatorial molecular plane that exhibits a high propensity for self-assembling into flat hydrogen-bonded two-dimensional nets (Goldberg, 2002, 2005). It has been shown that the hydroxy substituents may engage readily in O—H···O—H supramolecular synthons, leading to the formation of extended multiporphyrin arrays. Suitable examples include the zinc-metallated porphyrin Zn–TOHPP platform (Goldberg *et al.*, 1995). In some cases, water species are incorporated into the hydrogen-bonding patterns, bridging neighbouring porphyrin units while preserving the two-dimensional connectivity scheme. In this study, we attempted to use free base TOHPP building blocks in reactions with heavy metal ions as possible interporphyrin connectors under solvothermal conditions, following our earlier successful results to this end with the tetra(4-carboxyphenyl)porphyrin (TCPP) isomer (Goldberg, 2008). These reactions were carried out in a dimethylformamide–water or dimethylacetamide–water solvent environment, as hydrolysis of the amide was found to promote the synthesis of metal–organic frameworks (Burrows *et al.*, 2005; Lipstman *et al.*, 2007; Muniappan *et al.*, 2007). These solvent mixtures are then capable of solubilizing the TOHPP and engaging it in the supramolecular reaction. On the other hand, it is also well documented that the networking of functionalized porphyrin molecules, both *via* direct intermolecular hydrogen bonding or by intercoordination through bridging metal ions, can be disrupted readily by competing solvation that may prevent supramolecular association. This is common with strong Lewis base reagents, for example, dimethylformamide, dimethyl sulfoxide and pyridine, which have rather strong proton affinity for the hydroxy H atom (Lipstman *et al.*, 2006; George *et al.*, 2006). Indeed, present efforts to prepare TOHPP-based extended supramolecular architectures, either by O—H···O—H or O—H···metal···O—H interactions, under the given experimental conditions have failed. Instead, the products obtained represent totally solvated discrete porphyrin–solvent assemblies, held together by hydrogen bonds between the tetradentate porphyrin and the surrounding components, rather than extended network arrays. Similar observations have been reported for the TCPP platform (Lipstman *et al.*, 2006; George *et al.*, 2006).

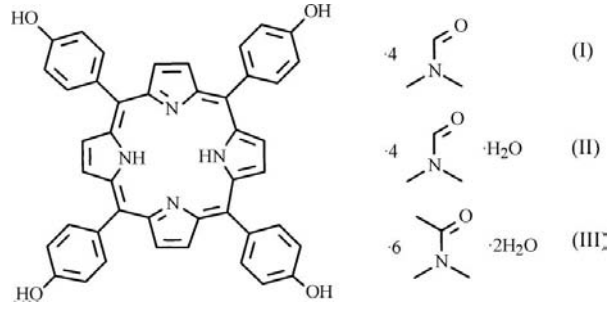

Within the above context, we describe here the structures of the solid products obtained by crystallizing TOHPP from a mixture of dimethylformamide and water, *viz.* (I) and (II), and dimethylacetamide and water, *viz.* (III). The molecular structures of (I)–(III) are shown in Figs. 1–3, respectively. In all cases, various lanthanide salts were also present in the solvothermal reactors, but not incorporated into the crystalline products.

Although compounds (I) and (II) were obtained from crystallization mixtures of similar composition, they represent differently structured adducts. In (I), the TOHPP unit is hydrogen bonded at the four corners of its molecular framework to a dimethylformamide species, forming a pentameric assembly, without incorporation of any water molecule into the structure (Table 1). The asymmetric unit contains two such

 doi:10.1107/S0108270108040018

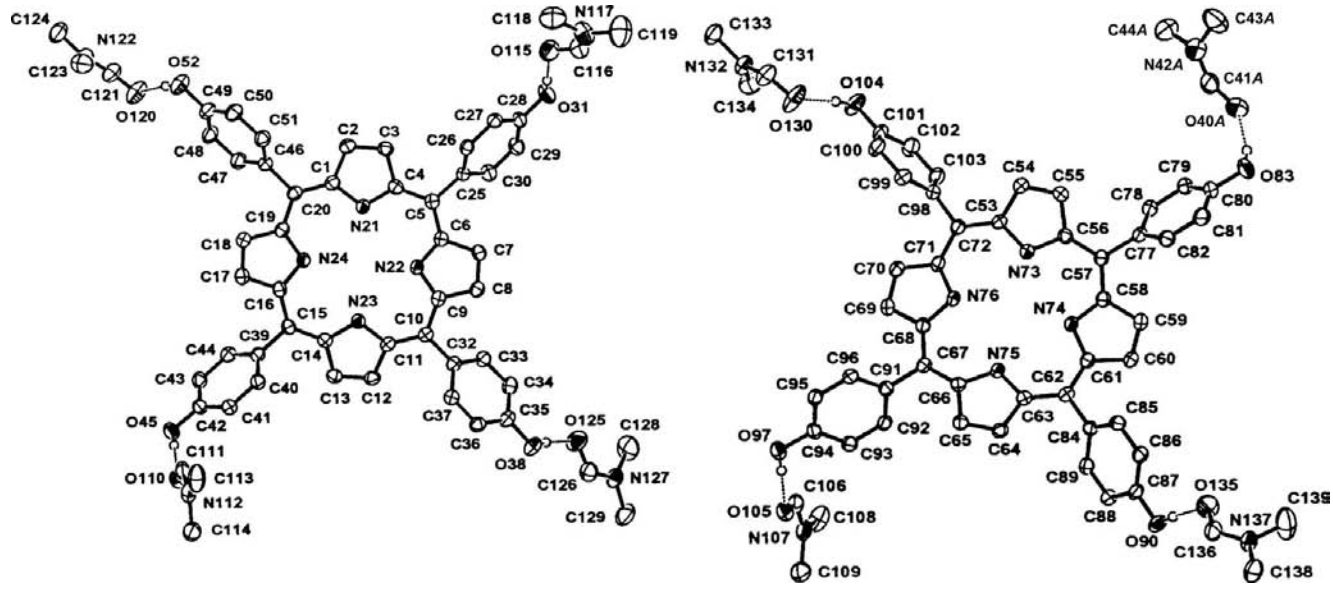

Figure 1
The molecular structure of compound (I), showing the atom-labelling schemes of the two crystallographically independent entities in the asymmetric unit. Displacement ellipsoids are drawn at the 50% probability level at *ca* 110 K. H atoms have been omitted, except for those involved in intermolecular hydrogen bonds (dotted lines). Only one orientation of the disordered dimethylformamide species is shown.

adduct assemblies of slightly different geometry and partial disorder of the terminal amide species (Fig. 1).

A different composition (TOHPP–dimethylformamide–water = 1:4:1) and connectivity scheme characterizes adduct (II). Here, only three of the OH groups (atoms O31, O45 and O52) form hydrogen bonds directly to the adjacent amide species, while the fourth hydroxyl site (atom O38) interacts with another amide molecule through an intervening water molecule (O73) (Fig. 2 and Table 2).

In (III), the porphyrin–dimethylacetamide–water composition is 1:6:2, and the entire nine-component hydrogen-bonded entity is located on an inversion centre (Fig. 3). The two inversion-related O26 hydroxyl groups form direct O—H···O(=C) hydrogen bonds with the amides. On the other hand, each of the O19 hydroxyl groups forms hydrogen bonds to a water molecule (O27) first, which then donates its two H atoms to the carbonyl groups of two other units of the dimethylacetamide, *viz.* atoms O28 and O34 (Table 3).

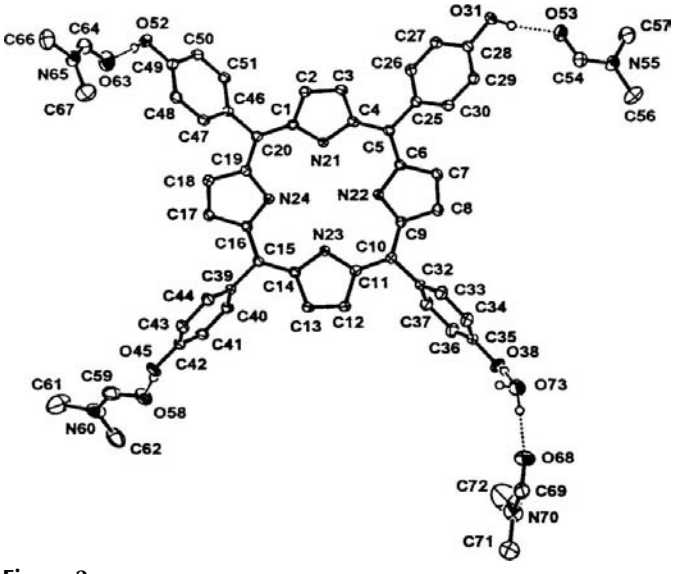

Figure 2
The molecular structure of compound (II), showing the atom-labelling schemes. Displacement ellipsoids are drawn at the 50% probability level at *ca* 110 K. H atoms have been omitted, except for those involved in intermolecular hydrogen bonds (dotted lines).

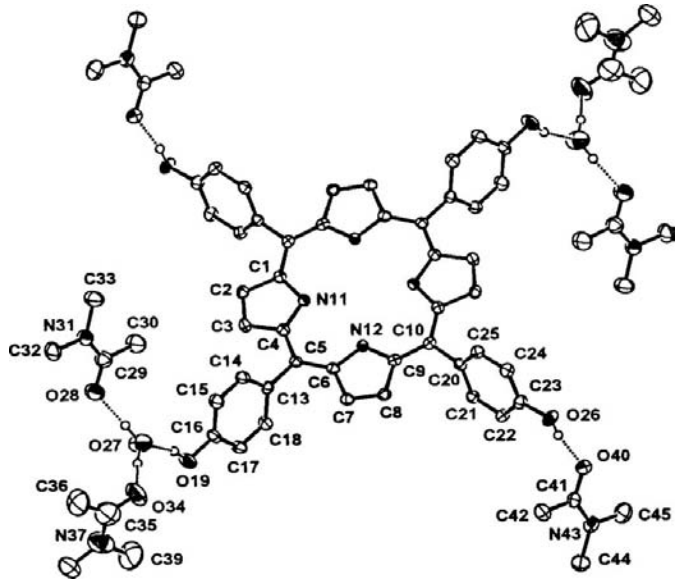

Figure 3
The molecular structure of compound (III), showing the atom-labelling scheme. The molecule resides on a crystallographic inversion centre, and only the asymmetric unit is labelled. Displacement ellipsoids are drawn at the 50% probability level at *ca* 110 K. H atoms have been omitted, except for those involved in intermolecular hydrogen bonds (dotted lines).

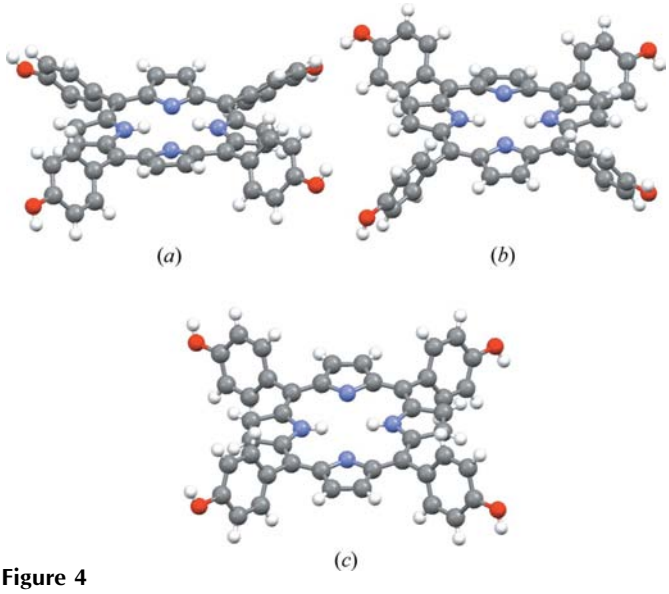

Figure 4
Ball-and-stick representations of the porphyrin molecules in (*a*) (I) (only one of the two units is shown, as both have very similar conformations), (*b*) (II) and (*c*) (III). The figures show the saddle-type distortion of the porphyrin cores from planarity in (I) and (II), and to a lesser extent in (III), which is required to minimize repulsion between the inner pyrrole H atoms.

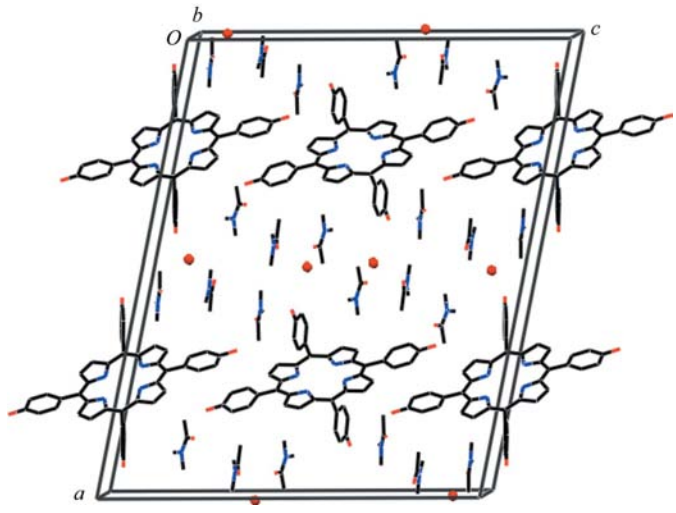

Figure 5
The crystal structure of (III). Water molecules are indicated by small spheres. H atoms have been omitted. Note the segregation between the porphyrin and solvent zones in the structure.

As expected, the conformation of the free base porphyrin macrocycle is significantly distorted from planarity in spite of its aromatic nature. This should be attributed to the repulsion between the inner pyrrole H atoms. In (I) and (II), a marked saddle-type distortion from planarity characterizes the conformation of the porphyrin core (Figs. 4*a* and 4*b*). A somewhat smaller distortion is observed in (III), but it is still evident from Fig. 4(*c*) that the inner pyrrole H atoms avoid each other as much as possible. The inner pyrrole H atoms could not be located from experimental data, which prevents a detailed discussion of this feature. It can only be said that the observed deformations are such that the minimum distance between the two H atoms (with the assumed N—H 'X-ray' bond length of 0.88 Å) across the porphyrin core is at least 2.3 Å.

The observed crystal packing in compounds (I)–(III) is charateristic of the vast number of porphyrin 'sponges' and clathrates, whether of purely van der Waals or hydrogen-bonding-assisted types, reported previously (*e.g.* Byrn *et al.*, 1993, and references therein). It generally consists of alternating (columnar or layered) zones of offset-stacked porphyrin molecules and molecules of the solvent. This is nicely demonstrated in Fig. 5, which depicts an intercalating type of molecular organization in (III).

In summary, this study describes the effects of competing solvation on the self-assembly of TOHPP-type porphyrin building blocks by hydrogen bonding, where solvent components bearing dominant (in the amide entities) or comparable (in the water solvent) H-atom-accepting capacity interfere with the direct assembly of the porphyrin units into supramolecular porphyrin arrays. It also reports for the first time crystal structures of the free base TOHPP entity.

Experimental

TOHPP and all reagents and solvents were obtained commercially. For the preparation of (I), TOHPP (3.1 mg, 0.005 mmol) was dissolved in dimethylformamide (DMF; 2.2 ml). To this, a solution of gadolinium(III) nitrate hexahydrate (9.0 mg, 0.020 mmol) in distilled water (1 ml) was added. The reaction mixture was heated in a sealed reactor to 443 K for 50 h, and then cooled slowly (at a rate of 0.5 K every 5 min) to ambient temperature, yielding a clear purple solution. A few drops of ethyl acetate were added and the solution allowed to evaporate slowly. X-ray quality (4 cm long) crystals were obtained after one month. For the preparation of (II), TOHPP (4.2 mg, 0.006 mmol) was dissolved in DMF (2.4 ml). To this, a solution of the gadolinium salt (8.4 mg, 0.019 mmol) in water (0.8 ml) was added. The reaction mixture was handled under solvothermal conditions exactly as described above. A few drops of pyridine were added to the resulting clear purple solution, which was then allowed to evaporate slowly. Rather large X-ray quality crystals were obtained after two months. For the preparation of (III), TOHPP (2.9 mg, 0.004 mmol) was dissolved in dimethylacetamide (2 ml). To this, the gadolinium salt (5.8 mg, 0.013 mmol) and triethylamine (1.2 ml) were added. The reaction mixture was placed in a sealed reactor and heated to 423 K for 50 h. After gradual cooling to ambient conditions, the resulting cloudy red–purple solution was filtered and a few drops of ethyl acetate were added. Slow evaporation of the solution over a period of two months yielded large X-ray quality crystals.

Compound (I)

Crystal data

$C_{44}H_{30}N_4O_4\cdot4C_3H_7NO$
M_r = 971.10
Triclinic, $P\overline{1}$
a = 13.6255 (2) Å
b = 16.0184 (3) Å
c = 26.2466 (5) Å
α = 101.7445 (12)°
β = 92.4786 (12)°
γ = 114.9158 (8)°
V = 5032.65 (15) Å^3
Z = 4
Mo $K\alpha$ radiation
μ = 0.09 mm^{-1}
T = 110 (2) K
0.40 × 0.40 × 0.20 mm

Table 1
Hydrogen-bond geometry (Å, °) for (I).

D—H···A	D—H	H···A	D···A	D—H···A
O31—H31···O115	0.84	1.80	2.6366 (18)	177
O38—H38···O125	0.84	1.82	2.6491 (17)	171
O45—H45···O110	0.84	1.83	2.6666 (16)	174
O52—H52···O120	0.84	1.83	2.6686 (18)	175
O83—H83···O40*A*	0.84	1.82	2.642 (4)	166
O83—H83···O40*B*	0.84	1.89	2.647 (4)	149
O90—H90···O135	0.84	1.86	2.6929 (18)	174
O97—H97···O105	0.84	1.81	2.6467 (16)	174
O104—H104···O130	0.84	1.86	2.6961 (18)	174

Table 2
Hydrogen-bond geometry (Å, °) for (II).

D—H···A	D—H	H···A	D···A	D—H···A
O31—H31···O53	0.84	1.87	2.6891 (18)	166
O38—H38···O73	0.84	1.88	2.720 (2)	175
O45—H45···O58	0.84	1.82	2.649 (2)	168
O52—H52···O63	0.84	1.80	2.6356 (19)	176
O73—H73*B*···O68	0.89	1.89	2.779 (2)	180
O73—H73*A*···O58^{i}	0.89	2.01	2.896 (2)	180

Symmetry code: (i) $x, y+1, z$.

Table 3
Hydrogen-bond geometry (Å, °) for (III).

D—H···A	D—H	H···A	D···A	D—H···A
O19—H19···O27	0.84	1.82	2.636 (3)	164
O26—H26···O40	0.84	1.79	2.618 (3)	168
O27—H27*A*···O28	0.91	1.77	2.681 (3)	177
O27—H27*B*···O34	0.96	1.81	2.745 (4)	166

Data collection

Nonius KappaCCD area-detector diffractometer
50610 measured reflections
23879 independent reflections
13053 reflections with $I > 2\sigma(I)$
$R_{int} = 0.051$

Refinement

$R[F^2 > 2\sigma(F^2)] = 0.063$
$wR(F^2) = 0.169$
$S = 1.04$
23877 reflections
1370 parameters
18 restraints
H-atom parameters constrained
$\Delta\rho_{max} = 0.36$ e Å^{-3}
$\Delta\rho_{min} = -0.39$ e Å^{-3}

Compound (II)

Crystal data

$C_{44}H_{30}N_4O_4\cdot 4C_3H_7NO\cdot H_2O$
$M_r = 989.12$
Triclinic, $P\overline{1}$
$a = 12.8346$ (2) Å
$b = 13.6669$ (2) Å
$c = 15.3200$ (3) Å
$\alpha = 102.8305$ (6)°
$\beta = 90.2339$ (6)°
$\gamma = 104.3547$ (11)°
$V = 2533.39$ (7) Å^3
$Z = 2$
Mo $K\alpha$ radiation
$\mu = 0.09$ mm^{-1}
$T = 110$ (2) K
0.60 × 0.50 × 0.30 mm

Data collection

Nonius KappaCCD area-detector diffractometer
26977 measured reflections
12018 independent reflections
8881 reflections with $I > 2\sigma(I)$
$R_{int} = 0.030$

Refinement

$R[F^2 > 2\sigma(F^2)] = 0.053$
$wR(F^2) = 0.153$
$S = 1.03$
12018 reflections
670 parameters
H-atom parameters constrained
$\Delta\rho_{max} = 0.48$ e Å^{-3}
$\Delta\rho_{min} = -0.44$ e Å^{-3}

Compound (III)

Crystal data

$C_{44}H_{30}N_4O_4\cdot 6C_4H_9NO\cdot 2H_2O$
$M_r = 1237.48$
Monoclinic, $C2/c$
$a = 35.5243$ (8) Å
$b = 6.5265$ (2) Å
$c = 29.2172$ (9) Å
$\beta = 102.2713$ (10)°
$V = 6619.2$ (3) Å^3
$Z = 4$
Mo $K\alpha$ radiation
$\mu = 0.09$ mm^{-1}
$T = 110$ (2) K
0.50 × 0.15 × 0.15 mm

Data collection

Nonius KappaCCD area-detector diffractometer
16577 measured reflections
6116 independent reflections
4359 reflections with $I > 2\sigma(I)$
$R_{int} = 0.050$

Refinement

$R[F^2 > 2\sigma(F^2)] = 0.069$
$wR(F^2) = 0.154$
$S = 1.03$
6116 reflections
418 parameters
H-atom parameters constrained
$\Delta\rho_{max} = 0.78$ e Å^{-3}
$\Delta\rho_{min} = -0.48$ e Å^{-3}

C-bound H atoms were located in calculated positions and constrained to ride on their parent atoms, with C—H = 0.95 or 0.98 Å and $U_{iso}(H) = 1.2$ or $1.5U_{eq}(C)$. O-bound H atoms were either located in difference Fourier maps or placed in calculated positions to correspond to idealized hydrogen-bonding geometries, with O—H = 0.84 Å for porphyrin O atoms or O—H = 0.89–0.96 Å for water O atoms. Their atomic positions were not refined, and they were constrained to ride on their parent atoms, with $U_{iso}(H) = 1.5U_{eq}(O)$. In (I), some of the dimethylformamide components are disordered, namely the O115- and O40-containing molecules. The methyl C atoms of the former species show large-amplitude displacement parameters, while the latter moiety reveals a twofold orientational disorder. DELU restraints (*SHELXL97*; Sheldrick, 2008) were applied to the displacement parameters of atoms O40/C41/N42/C43/C44, and DFIX restraints (*SHELXL97*) were applied to the N117—C118 and N117—C119 bonds. Restraint-free least-squares refinements were applied to structures (II) and (III). In all three structures, the two N-bound H atoms within the porphyrin core could not be located reliably. As some residual electron density was observed near all the pyrrole N atoms, the H atoms bound to them were assumed to be disordered equally between the four pyrrole rings and were located in calculated positions, with N—H = 0.88 Å and $U_{iso}(H) = 1.2U_{eq}(N)$.

For all three title compounds, data collection: *COLLECT* (Nonius, 1999); cell refinement: *DENZO* (Otwinowski & Minor, 1997); data reduction: *DENZO*; program(s) used to solve structure: *SHELXS97* (Sheldrick, 2008) for (I); *SIR97* (Altomare *et al.*, 1994) for (II) and (III); program(s) used to refine structure: *SHELXL97* (Sheldrick, 2008); molecular graphics: *ORTEPIII* (Burnett & Johnson, 1996) and *Mercury* (Macrae *et al.*, 2006); software used to prepare material for publication: *SHELXL97*.

This research was supported in part by the Israel Science Foundation.

Supplementary data for this paper are available from the IUCr electronic archives (Reference: GD3260). Services for accessing these data are described at the back of the journal.

References

Altomare, A., Cascarano, G., Giacovazzo, C., Guagliardi, A., Burla, M. C., Polidori, G. & Camalli, M. (1994). *J. Appl. Cryst.* **27**, 435.

Burnett, M. N. & Johnson, C. K. (1996). *ORTEPIII*. Report ORNL-6895. Oak Ridge National Laboratory, Tennessee, USA.

Burrows, A. D., Cassar, K., Friend, R. M. W., Mahon, M. F., Rigby, S. P. & Warren, J. E. (2005). *CrystEngComm*, **7**, 548–550.

Byrn, M. P., Curtis, C. J., Hsiou, Y., Khan, S. I., Sawin, P. A., Tendick, S. K., Terzis, A. & Strouse, C. E. (1993). *J. Am. Chem. Soc.* **115**, 9480–9497.

George, S., Lipstman, S., Muniappan, S. & Goldberg, I. (2006). *CrystEngComm*, **8**, 417–424.

Goldberg, I. (2002). *CrystEngComm*, **4**, 109–116.

Goldberg, I. (2005). *Chem. Commun.* pp. 1243–1254.

Goldberg, I. (2008). *CrystEngComm*, **10**, 637–645.

Goldberg, I., Krupitsky, H., Stein, Z., Hsiou, Y. & Strouse, C. E. (1995). *Supramol. Chem.* **4**, 203–221.

Lipstman, S., Muniappan, S., George, S. & Goldberg, I. (2006). *CrystEngComm*, **8**, 601–607.

Lipstman, S., Muniappan, S., George, S. & Goldberg, I. (2007). *Dalton Trans.* pp. 3273–3281.

Macrae, C. F., Edgington, P. R., McCabe, P., Pidcock, E., Shields, G. P., Taylor, R., Towler, M. & van de Streek, J. (2006). *J. Appl. Cryst.* **39**, 453–457.

Muniappan, S., Lipstman, S., George, S. & Goldberg, I. (2007). *Inorg. Chem.* **46**, 5544–5554.

Nonius (1999). *COLLECT*. Nonius BV, Delft, The Netherlands.

Otwinowski, Z. & Minor, W. (1997). *Methods in Enzymology*, Vol. 276, *Macromolecular Crystallography*, Part A, edited by C. W. Carter Jr & R. M. Sweet, pp. 307–326. New York: Academic Press.

Sheldrick, G. M. (2008). *Acta Cryst.* A**64**, 112–122.